

WISCO

UNIVERSITY OF WISCONSIN • MADISON, WISCONSIN

PLASMA PHYSICS

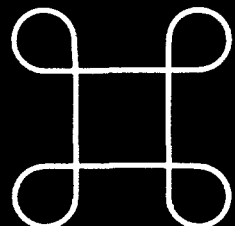
40
11/19/96
J.S. 2

IMPURITIES, TEMPERATURE, AND DENSITY IN A MINATURE
ELECTROSTATIC PLASMA AND CURRENT SOURCE

D.J. Den Hartog, D.J. Craig, G. Fiksel[†], and J.S. Sarff[†]

DOE/ER/54345-284

October 1996



WISCONSIN

NOTICE

This report was prepared as an account of work sponsored by an agency of the United States Government. Neither the United States nor any agency thereof, nor any of their employees, makes any warranty, expressed or implied, or assumes any legal liability or responsibility for any third party's use or the results of such use of any information, apparatus, product or process disclosed in this report, or represents that its use by such third party would not infringe privately owned rights.

Printed in the United States of America
Available from
National Technical Information Service
U.S. Department of Commerce
5285 Port Royal Road
Springfield, VA 22161

NTIS Price codes
Printed copy: A02
Microfiche copy: A01

DISCLAIMER

This report was prepared as an account of work sponsored by an agency of the United States Government. Neither the United States Government nor any agency thereof, nor any of their employees, makes any warranty, express or implied, or assumes any legal liability or responsibility for the accuracy, completeness, or usefulness of any information, apparatus, product, or process disclosed, or represents that its use would not infringe privately owned rights. Reference herein to any specific commercial product, process, or service by trade name, trademark, manufacturer, or otherwise does not necessarily constitute or imply its endorsement, recommendation, or favoring by the United States Government or any agency thereof. The views and opinions of authors expressed herein do not necessarily state or reflect those of the United States Government or any agency thereof.

DISCLAIMER

**Portions of this document may be illegible
in electronic image products. Images are
produced from the best available original
document.**

Impurities, Temperature, and Density in a Miniature Electrostatic Plasma and Current Source

D J Den Hartog and D J Craig

Department of Physics, University of Wisconsin—Madison, 1150 University Avenue, Madison, Wisconsin 53706, U.S.A.

G Fiksel and J S Sarff

Sterling Scientific, Inc., 1415 Rutledge Street, Madison, Wisconsin 53703, U.S.A.

ABSTRACT

We have spectroscopically investigated the Sterling Scientific miniature electrostatic plasma source—a plasma gun. This gun is a clean source of high density (10^{19} - 10^{20} m⁻³), low temperature (5 - 15 eV) plasma. A key result of our investigation is that molybdenum from the gun electrodes is largely trapped in the internal gun discharge; only a small amount escapes in the plasma flowing out of the gun. In addition, the gun plasma parameters actually improve (even lower impurity contamination and higher ion temperature) when up to 1 kA of electron current is extracted from the gun via the application of an external bias. This improvement occurs because the internal gun anode no longer acts as the current return for the internal gun discharge. The gun plasma is a virtual plasma electrode capable of sourcing an electron emission current density of 1 kA/cm². The high emission current, small size (3 - 4 cm diameter), and low impurity generation make this gun attractive for a variety of fusion and plasma technology applications.

1. INTRODUCTION

The Sterling Scientific plasma gun is capable of producing a clean, high density ($10^{19} - 10^{20} \text{ m}^{-3}$), low temperature ($T_i \approx T_e \approx 5 - 15 \text{ eV}$) plasma for pulse lengths of at least 40 ms. With the addition of a bias electric field, it is a high current emission source (1 kA) at high current density (1kA/cm^2). A schematic of a typical source assembly is shown in Fig. 1a. The heart of the source is a set of electrodes used to form a small, cylindrical arc discharge plasma column. The principal electrodes are the anode and cathode. In addition to these, a stack of washers is used to define the arc channel between the anode and cathode. The washer stack is composed of alternating insulating and (electrically isolated) metal washers. Washers are used to minimize the plasma contact with material surfaces while providing a partial conducting boundary to help stabilize the plasma column. (The insulating washers have larger inner diameter than the metal washers and do not significantly contact plasma.) The source is very reproducible and reliable with metal washers, whereas it can become erratic with only insulating washers. This design represents the evolution of earlier designs using the same basic concepts [1,2].

Spectroscopic investigation of the gun plasma had two major purposes. The first was to identify the major impurities and determine their behavior, both within the internal gun discharge and in the plasma flowing out of the gun. The second was to determine ion and neutral temperatures (T_i and T_n) and ion density (n_i) via Doppler and Stark broadening respectively. A key result is the observation that there appears to be only a very small amount of molybdenum (from the gun electrodes) in the hydrogen plasma flowing out of the gun when it is optimally operated. In addition, the gun plasma parameters actually improve (lower impurity contamination and higher T_i) when current is extracted from the gun. These results confirm the hypothesis that the gun plasma acts as a “virtual electrode” during current extraction.

The spectrometer used for this work was specifically designed and built to diagnose the gun plasma [3]. It is fiber optically coupled and equipped with a computer controlled CCD detector. This instrument is capable of both high resolution ($\Delta\lambda \leq 0.015 \text{ nm}$) for line broadening measurements and large bandpass (110 nm with $\Delta\lambda \sim 0.3 \text{ nm}$) for impurity surveys. Most of spectroscopic data presented below was taken from one of two chordal views of the plasma (Fig. 1). The “end view” was

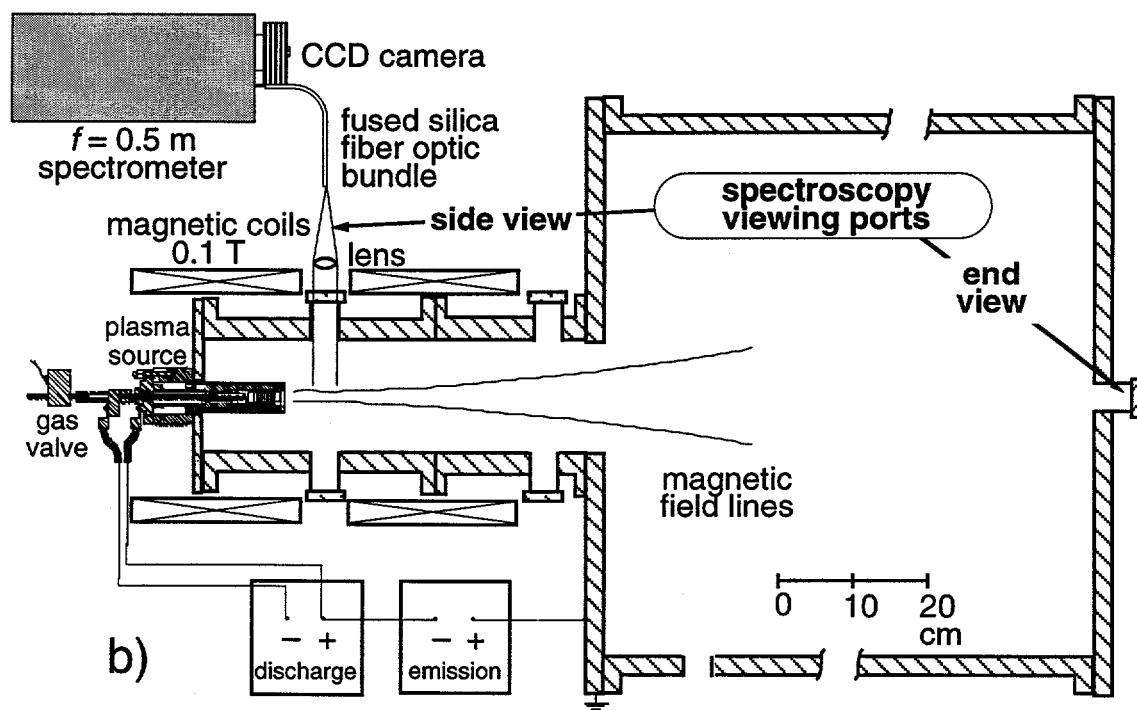
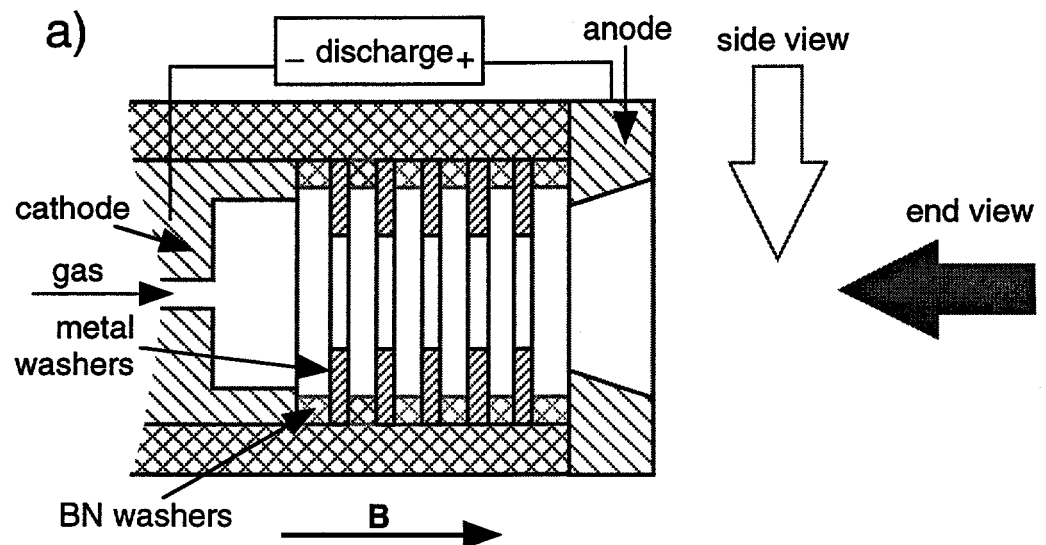


Fig. 1. Overall view of the a) plasma source and b) test chamber, including placement of the side and end views used for spectroscopic measurements.

aligned with the axis of the gun discharge and viewed it directly through the hole in the anode. The “side view” was perpendicular to the axis of the gun discharge and viewed the plasma flowing out of the gun, about 5 cm past the gun anode.

2. IMPURITY SURVEY

2.1 Bright emission lines

Table I is a catalog of the bright ultraviolet and visible emission lines identified in the variety of gun plasmas that were produced. Fig. 2 shows typical spectra from 200 to 300 nm and 300 to 400 nm. The low Z impurities boron, carbon, and nitrogen come mostly from the boron nitride spacer washers inside the gun, while the metal impurities come from the internal gun electrodes and metal spacer washers. The bright lines observed all came from neutral to doubly ionized impurity ions. More highly ionized species did not appear to be present; the bright triplets of B IV at 282 nm and C V at 227 nm were notably absent even though the electron temperature (5 to 20 eV, depending on gun operation) was high enough to produce such ions. We speculate that particle confinement time in the gun plasma is not long enough to allow the impurities to reach the more highly ionized states.

Species	Bright lines (nm)
H I	434.047, 486.133, 656.3
B II	345.129
B III	206.578, 206.723
C II	283.671, 283.760, 514.516
C III	229.687
N II	500.515, 567.956
Cu I	324.754, 327.396
Cu II	224.700
Mo I	379.825, 386.411, 390.296
Mo II	281.615, 281.744
Mo III	233.093

Table I. Bright UV and visible emission lines in gun plasmas

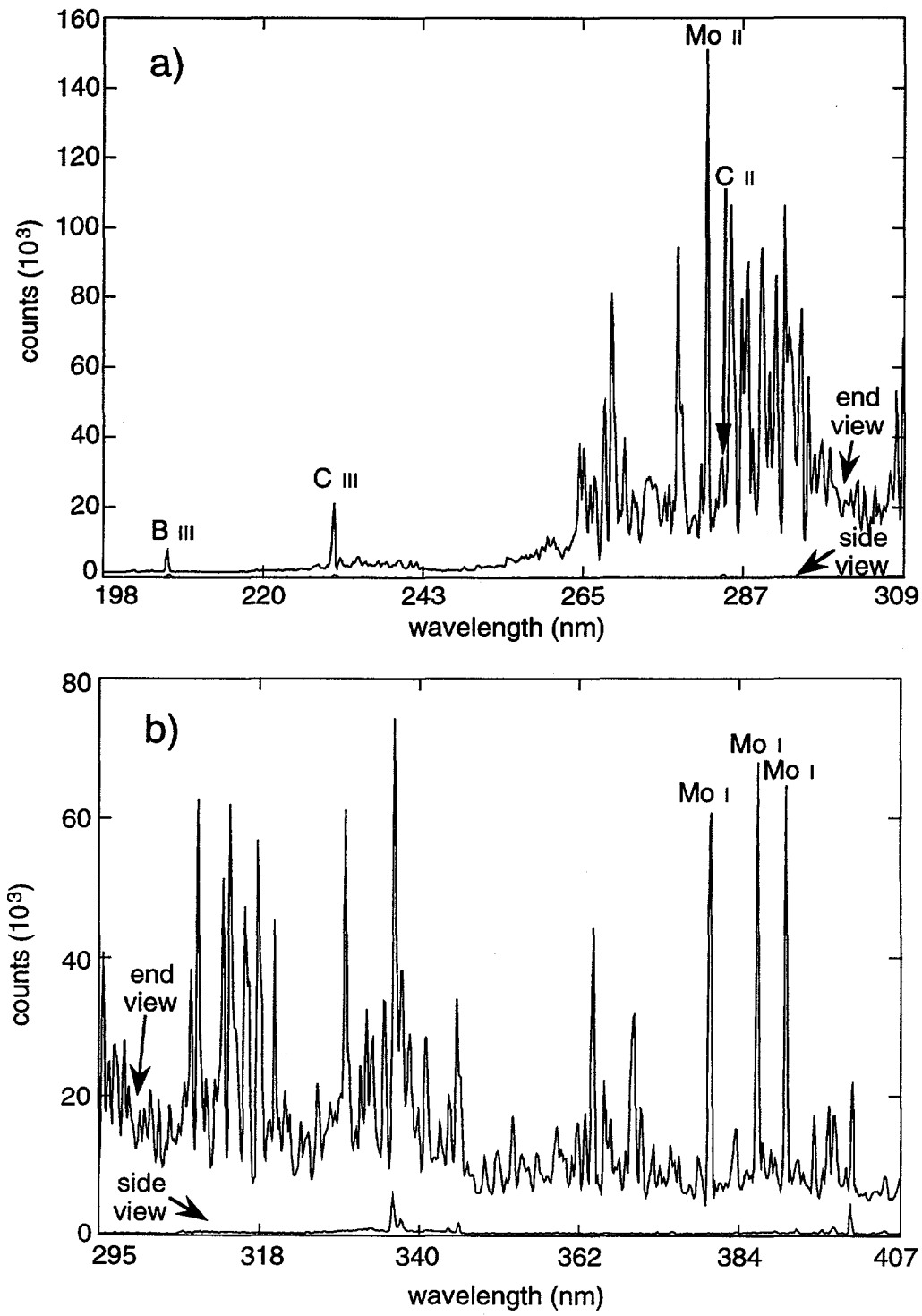


Fig. 2. Comparison of relative impurity levels in the internal gun plasma (end view) and plasma flowing out of the gun (side view). a) Spectrum from 200 to 300 nm, b) from 300 to 400 nm.

The majority of gun operation has been with molybdenum electrodes and washers; it was operated with copper electrodes and washers for a short time to quantify how deleterious the increased sputtering coefficient of copper was to gun operation. Most of the data presented in this section was taken by integrating (with the CCD detector) the line emission over the entire gun discharge. A single monochromator with a photomultiplier tube was also used to measure the time variation of a few specific lines during a gun discharge.

2.2 Molybdenum electrode guns

Several different molybdenum electrode gun configurations were examined spectroscopically, but no large difference in the behavior of impurities was observed. Instead, the most striking result is the substantial difference in character between the spectra recorded with the end view from those recorded with the side view (Fig. 2). All of the impurity features are greatly suppressed in the side view compared to the end view. In particular, note that the Mo I and Mo II lines are not even visible on the side view spectra in Fig. 2, while the same lines are clearly apparent in the end view. Some of this difference is due to the fact that the end viewing chord integrates over the emission from a much larger volume of plasma than the side viewing chord. The plasma inside the gun seen by the end view is also more dense than that seen by the side view. The magnitude of these effects can be roughly estimated by comparing the ratios of the H_B, B III, C II, and C III line emission from the side view to that from the end view. These ratios are typically about 10%, implying that Mo line emission seen by the side view could be reasonably expected to be about 10% of that seen by the end view. In fact, the Mo I emission is $\leq 0.5\%$ of that seen by the end view, while the upper bound on the Mo II emission ratio is even smaller ($\leq 0.2\%$). There are at least two non-exclusive explanations for this behavior. First, sputtering of molybdenum may be more severe at the gun cathode than the anode because the cathode suffers ion bombardment while the anode draws only electron current. Thus the plasma surrounding the cathode (which is clearly seen by the spectrometer in the end view) may be more heavily contaminated since it is close to the source of molybdenum. Second, the molybdenum in the internal gun plasma may be partly “trapped” so that it does not flow out of the gun with the external plasma stream. This trapping at the cathode may be simply that most of the molybdenum atoms sputtered off the cathode quickly ionize and fall back onto the cathode.

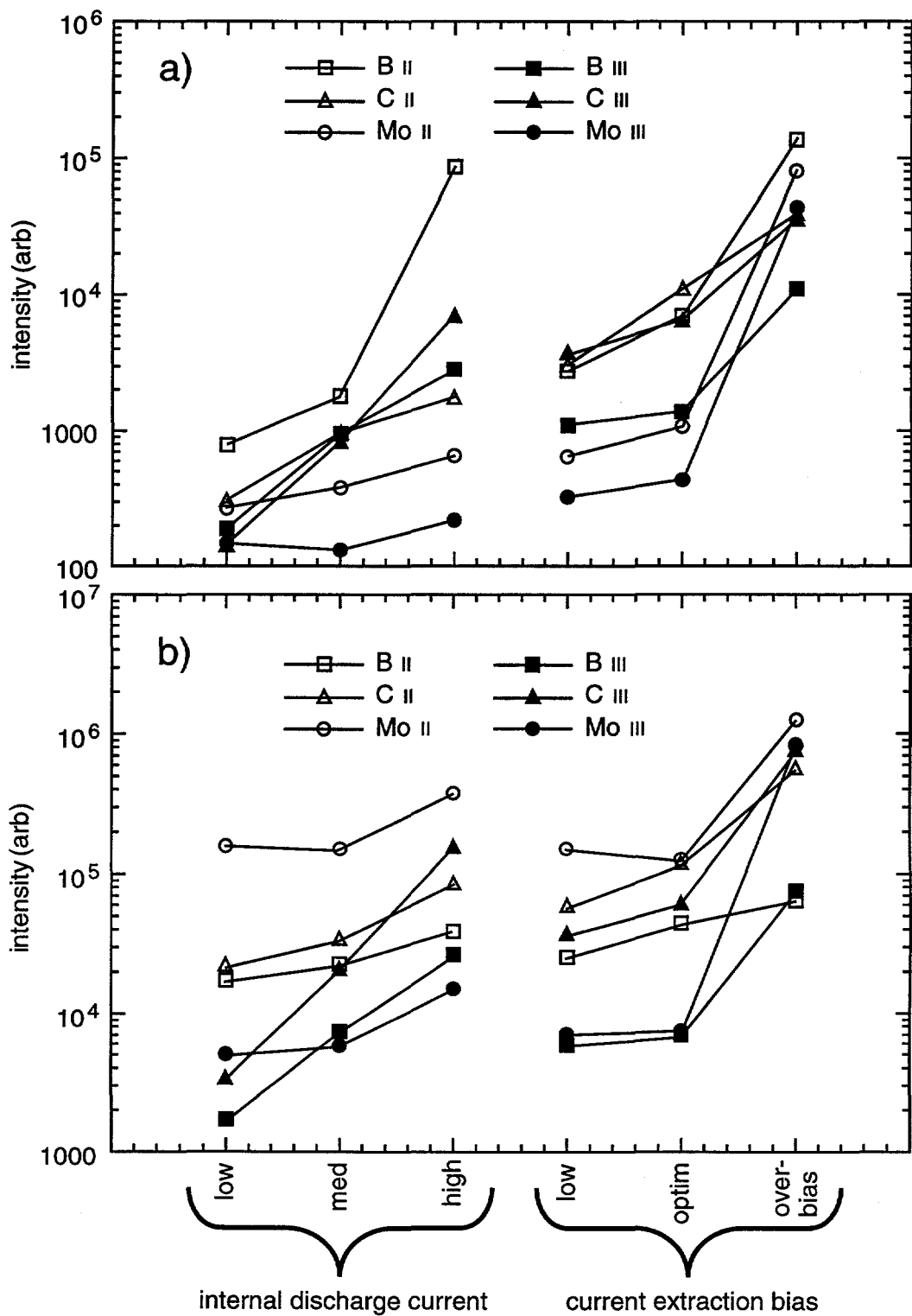


Fig. 3. Comparison of impurity line emission intensity while varying internal gun discharge current and current extraction bias. a) Side view and b) end view.

Operation of the plasma gun can be degraded if too much current is forced to flow in the internal discharge and/or if too little hydrogen gas is supplied to fuel this discharge. When the gun is operated is operated in these conditions, the overall level of impurity line emission increases and can become very large if the discharge is severely undergassed or if the internal current density greatly exceeds 1 kA/cm^2 (this may be the current density limit for this type of gun).

When the plasma gun is operated as an electron current source by application of a voltage bias between the gun and some distant current collector (e.g., a vacuum vessel wall), the plasma inside the gun acts as a virtual electrode. This type of operation does not raise impurity contamination of the the plasma and may actually lower impurity contamination below that achieved during operation of the gun as a simple plasma source. Figure 3 contains a comparison of impurity line emission intensity obtained during "biased" operation (electron current being extracted) and "unbiased" operation. The first three sets of datapoints on the left side of the graphs are from unbiased operation of the gun; optimum discharge current of about 1000 A lies between the point at medium current point at 820 A and the high current point at 1120 A. Note that impurity contamination of the plasma begins to rise significantly at the high discharge current. The second set of three datapoints on the right side of the graphs are from biased operation of the gun, with the internal discharge current at the optimum of about 1000 A. In general, impurity levels decrease or remain unchanged at the low (40 V, 550 A) and optimum (85 V, 900 A) bias settings, but dramatically increase at the overbias point (115 V, 1030 A). Figure 4 clearly illustrates the change in character of the impurity spectra between optimum and overbiased cases. At optimum bias settings and below, the plasma in the internal discharge acts as a "virtual electrode;" the plasma is the source of the electron emission current extracted from the gun by the external bias. Beyond the optimum bias point the electron emission from the internal gun plasma saturates and all additional emission current comes directly from the metal electrodes in the gun (thus the large increase in the molybdenum lines as metal is sputtered from the surface). We speculate that the decrease in impurity line emission upon the application of bias is caused by the removal of the gun anode from the current return path. All of the electron current from the internal discharge is drawn out of the gun by the bias and returned through the vacuum vessel walls. This minimizes the interaction of the gun plasma with the anode surface and reduces impurity emission.

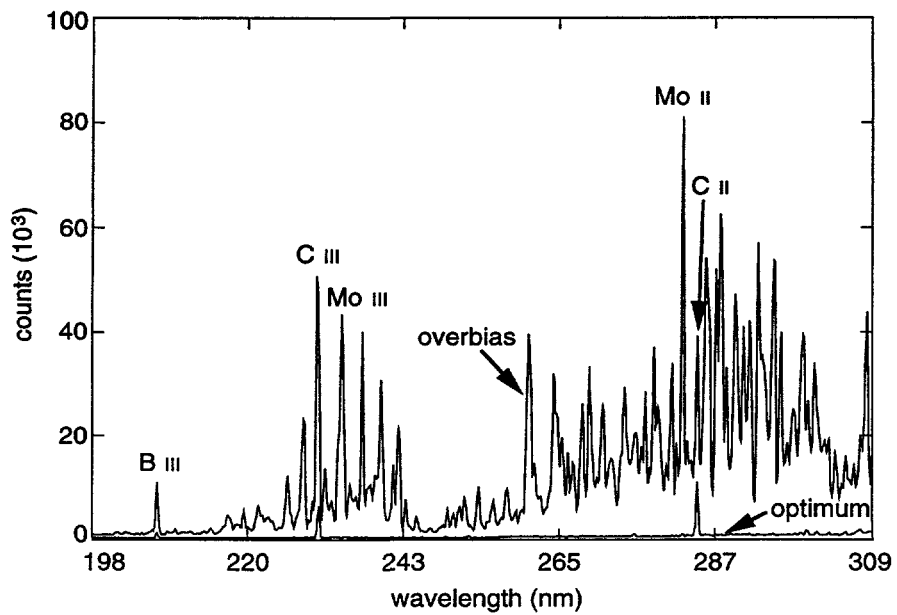


Fig. 4. Comparison of relative impurity levels with gun at optimum current extraction bias level (lower trace) and in "overbias" condition (upper trace). This data is from the side view position.

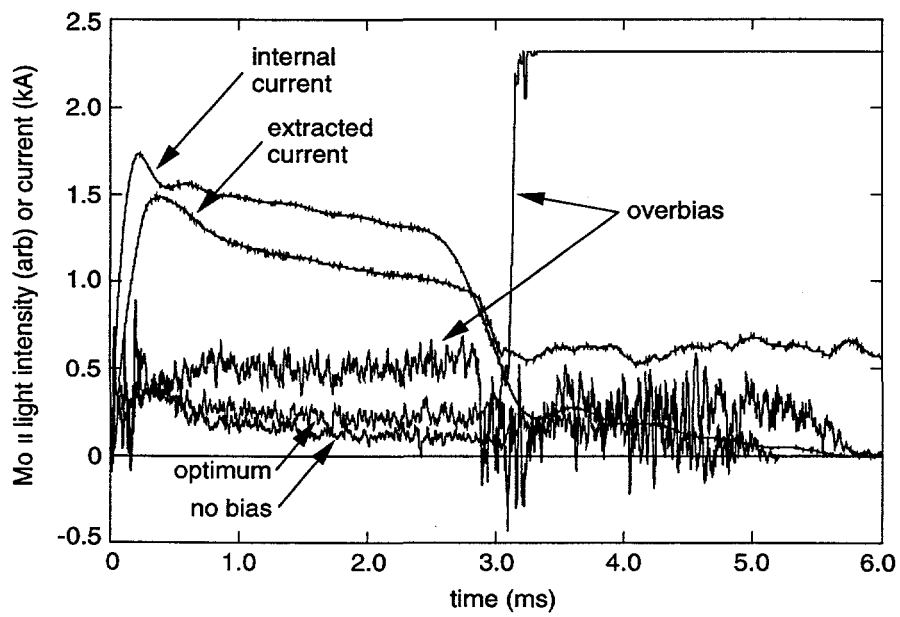


Fig. 5. Comparison of the Mo II light intensity for no current extraction bias on the plasma gun, optimum bias, and overbias. Also shown is the internal gun discharge current and extracted current for the overbias case.

2.3 Time variation of specific impurity lines

Examination of the time variation of specific impurity lines with a monochromator and photomultiplier tube reveals why “overbiasing” the gun beyond the plasma electron emission saturation point causes such a dramatic increase in impurity contamination of the gun plasma. Figure 5 shows Mo II line intensities for several gun discharges (Mo I and Mo III are similar), as recorded from the side view. The Mo II line intensity is very similar for the “no bias” and “optimum bias” discharges, but exhibits dramatically different behavior during the “overbiased” discharge. Upon termination of the internal gun current (which occurs at 3 ms and is controlled by a pulse forming network), the Mo II line intensity immediately saturates the detector during the overbiased case. Substantial “extracted current” also continues to flow beyond 3 ms. This does not occur in the unbiased or optimally biased cases. It seems reasonable to conclude that the extracted current that continues to flow after the internal gun discharge during the overbiased case is being drawing directly from the molybdenum anode of the plasma gun, rather than from the virtual electrode formed by the plasma inside the gun. In fact, this situation clearly illustrates the advantage of plasma virtual electrode over a real metal electrode. The virtual electrode provides clean emission of a high density electron current, whereas surface erosion of a metal electrode contaminates the plasma and surrounding surfaces and eventually results in electrode failure when sufficient erosion has occurred.

As the current extraction bias is raised, it may be possible to sensitively determine the point at which overbias is about to occur by spectroscopically monitoring the metal contamination of the plasma flowing out of the gun. Note from Fig. 5 that the Mo II emission intensity during the gun discharge (0 to 3 ms) is larger for the overbiased case than for optimum or no bias. This implies that some fraction of the extracted current is being drawn from the molybdenum anode even during the gun discharge, a situation that should be avoided since it leads to current extraction from the metal anode following the termination of the internal gun discharge. We have found that this problem can be somewhat mitigated by active control of the current extraction bias. If this bias is turned off immediately after the termination of the internal gun current, then large amounts of current will not be extracted from the molybdenum gun anode. However, such control does not prevent extraction of the

fraction of the current that is drawn from the molybdenum anode during the gun discharge; this can only be remedied by lowering the extraction bias to the optimum level.

2.4 Copper electrode gun

The molybdenum electrodes and washers in the plasma gun were replaced with copper equivalents for a short operational period. Copper differs from molybdenum in two important ways: 1) the thermal conductivity is higher and 2) the surface sputtering threshold is lower. Higher thermal conductivity of the electrodes and washers is advantageous in that the surface heat load generated by operation of the internal gun discharge can be drawn away and dissipated more effectively. However, an increase in erosion of the surface inevitably leads to increased impurity contamination of the plasma. Copper lines were observed to be bright in both the end and side views. Especially striking was the high relative brightness of these lines viewed from the side compared to the end. This is unlike the behavior of the molybdenum lines shown in Fig. 2, where the Mo I and Mo II lines are so weak in the side view that they are almost invisible. It is likely that the electron current drawn to the copper gun anode erodes significantly more metal than the same current drawn to a molybdenum anode. These copper ions are not trapped in the same way that metal ions are trapped at the cathode, but instead flow out of the gun with the plasma stream.

Visual inspection of the copper electrodes and washers following a total of approximately 100 3 ms gun pulses revealed that substantial erosion of all plasma facing surfaces had taken place. The same inspection of molybdenum components after thousands of gun pulses reveals minimal surface damage and erosion. We have concluded that the gun electrodes and washers must be made from a refractory metal with a low sputtering coefficient.

2.5 Conclusions

The major impurities in the gun plasma are boron, carbon, and nitrogen from the boron nitride spacer washers, and molybdenum from the electrodes and conducting washers. Only neutral to doubly ionized impurities were observed. Relatively little molybdenum contamination appears in the plasma flowing out of the gun; it appears to be largely trapped in the internal gun discharge. When the plasma gun is operated as an electron current source by application of a voltage bias between

the gun and some distant current collector, the plasma inside the gun acts as a virtual electrode. This type of operation actually appears to decrease impurity contamination of the plasma flowing out of the gun, probably because the gun anode ceases to act as the current return for the internal gun discharge. In contrast to a metal electrode, the virtual electrode formed by the plasma inside the gun provides clean emission of a high density electron current.

3. EMISSION LINE BROADENING

3.1 Thermal and Stark broadening

The two emission line broadening mechanisms useful for diagnosing the gun plasma are thermal and Stark broadening [4]. Thermal broadening arises from the Doppler shift caused by thermal particle motion, a Maxwellian velocity distribution giving rise to a Gaussian line profile. For a Maxwellian velocity distribution and a Gaussian instrument function, the resulting line profile is

$$I_G(\lambda) = I_o \exp \left[-\frac{(\lambda - \lambda_o)^2}{\Gamma_T^2 + \Gamma_I^2} \right]$$

where $1.665\Gamma_T$ is the FWHM of the Doppler profile and $1.665\Gamma_I$ is the FWHM of the Gaussian instrument function. Stark broadening, also called pressure or collisional broadening, arises from the influence (via electric field) of nearby ions upon the emitting atom (hydrogen, in this case). Stark broadening results in a Lorentzian line profile:

$$I_L(\lambda) = \frac{I_o}{1 + \left[(\lambda - \lambda_o) \frac{2}{\Gamma_L} \right]^2}$$

where Γ_L is the FWHM. For H_β , if Stark broadening is dominant, $\Gamma_L = 0.040n_i^{2/3}$ nm, with ion density in 10^{20} m^{-3} . Of course, in the gun plasma, the effects of thermal and Stark broadening are combined, so I_L and I_G must be convolved, resulting in a Voigt function:

$$I_V(\lambda) = I_o \int_{-\infty}^{+\infty} \frac{\exp(-y^2)}{\frac{I_L^2}{4(I_T^2 + I_I^2)} + \left(\frac{(\lambda - \lambda_o)}{\sqrt{I_T^2 + I_I^2}} - y \right)^2} dy$$

which has no analytic closed form, but can be approximated with the IDL [5] VOIGT function.

3.2 Diagnostic setup

The B III line at 206.578 nm was used to measure ion temperature in the gun plasma because it is intrinsically bright, the line profile is dominated by thermal broadening, and it is isolated from any interfering spectral lines. In addition, the B III ions, since they were the highest ionization state of boron observed, should be reflective of conditions in the the highest temperature region of the gun plasma. The impurity ion - majority ion equilibration time for this high density (10^{20} m^{-3}), low temperature (10 eV) plasma is short, approximately 1 μs . Even given what must be a very short particle confinement time in the gun plasma, the impurity ions should be near equilibrium to the majority species.

The H_β line at 486.133 nm was used to measure the ion density and, secondarily, the neutral atom temperature. It's likely that the H_β emission is not spatially localized but originates from the entire volume of the gun plasma and thus represents some sort of spatial average.

Two operational details should be mentioned. First, the B III line brightness was enhanced for this dataset by fitting the gun with a boron nitride spacer washer with a smaller inner diameter (similar to the inner diameter of the molybdenum washers, see Fig. 1a). This did not appear to affect operation of the gun. Second, the B III line profile was recorded by the spectrometer during the latter part of the gun discharge, skipping the first millisecond in order to avoid recording behavior during the period in which the boron was reaching ionization equilibrium. The H_β line emission was recorded over the entire 3 ms gun discharge, but care was taken to stop collecting light at the end of the discharge since the afterglow plasma that persisted 3 ms after the gun discharge produced a substantial amount of H_β light.

3.3 Ion temperature

Two important observations summarize the B III measurements: upon application of the current extraction bias, the ion temperature doubles and the line brightness drops significantly. The current extraction bias seems to both heat the

gun plasma and reduce the impurity level.

The specific results are illustrated in Fig. 6. The end view shows $T_{i\parallel}$ going from 12 to 24 eV upon the application of bias, while $T_{i\perp}$ from the side view goes from 7 to 15 eV. In both cases the line brightness recorded by the spectrometer dropped significantly upon the application of bias. This decrease does not appear to be simply an ionization to B IV, as the characteristic lines of that ion did not appear upon the application of bias. Some of the difference may be due to density changes in the plasma, but most likely it is simply a further indication that current extraction bias reduces the impurity content of the gun plasma by reducing interaction with the electrodes and washers.

Note that there appears to be a statistically significant enhancement of the light level in the spectrometer channels on the long-wavelength side of the end view Doppler broadened spectrum (Fig. 6). This feature was always present and was reproduced in the B III 206.723 nm line. It appears to be a manifestation of directed flow of ions (with about 10 eV of kinetic energy) away from the spectrometer and toward the gun cathode. Interestingly, this feature was most apparent in spectra taken in an "offset" end view (Fig. 7) in which the spectrometer was in the end view location, but was shifted very slightly to so as not to view the plasma in the internal gun discharge. This provided a view parallel to the applied magnetic field (and gun axis) of the plasma just outside of the gun anode. With this view, application of the current extraction bias noticeably reduced the size of the red-shift feature (unlike the regular end view, in which there was no difference between the bias and no-bias cases). Since this red-shift did not appear in the side view, it must be due to some potential drop parallel to the gun axis and magnetic field, but not necessarily the cathode fall inside the gun.

3.4 Neutral temperature and ion density

The results from measurements of the broadening of the H_β (Fig. 8) are not as easy to summarize. In general, the ion density is quite high, in the range of 10^{20} m^{-3} . This is in agreement with probe measurements of the plasma density [1]. The hydrogen neutral atom temperature is on the order of 1 eV.

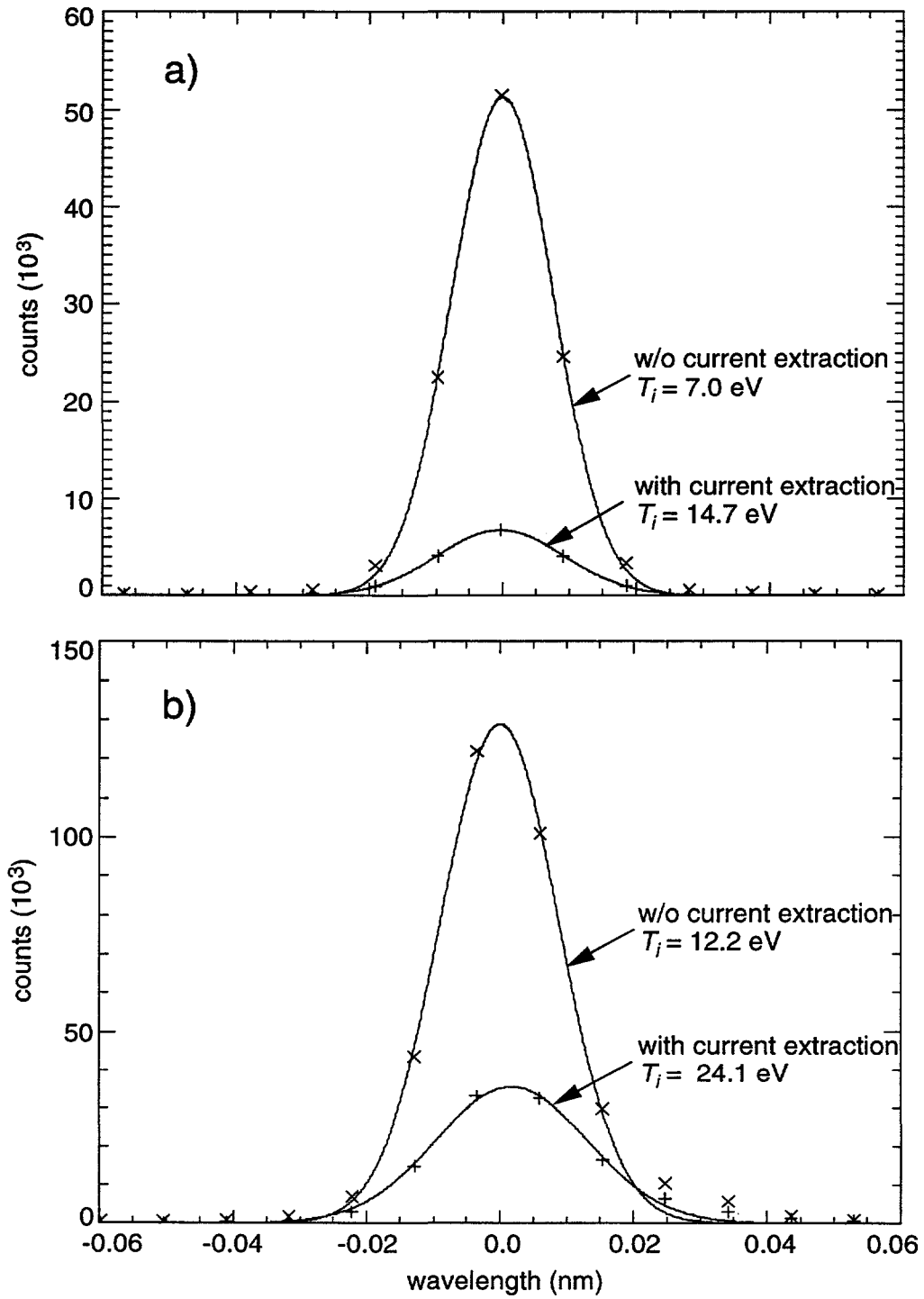


Fig. 6. Comparison of the Doppler broadened profiles of the 206.58 nm B III line from the a) side view and b) end view. With the current extraction bias turned on, the ion temperature doubles and the line intensity drops (indicative of a general decrease in the impurity content of the plasma).

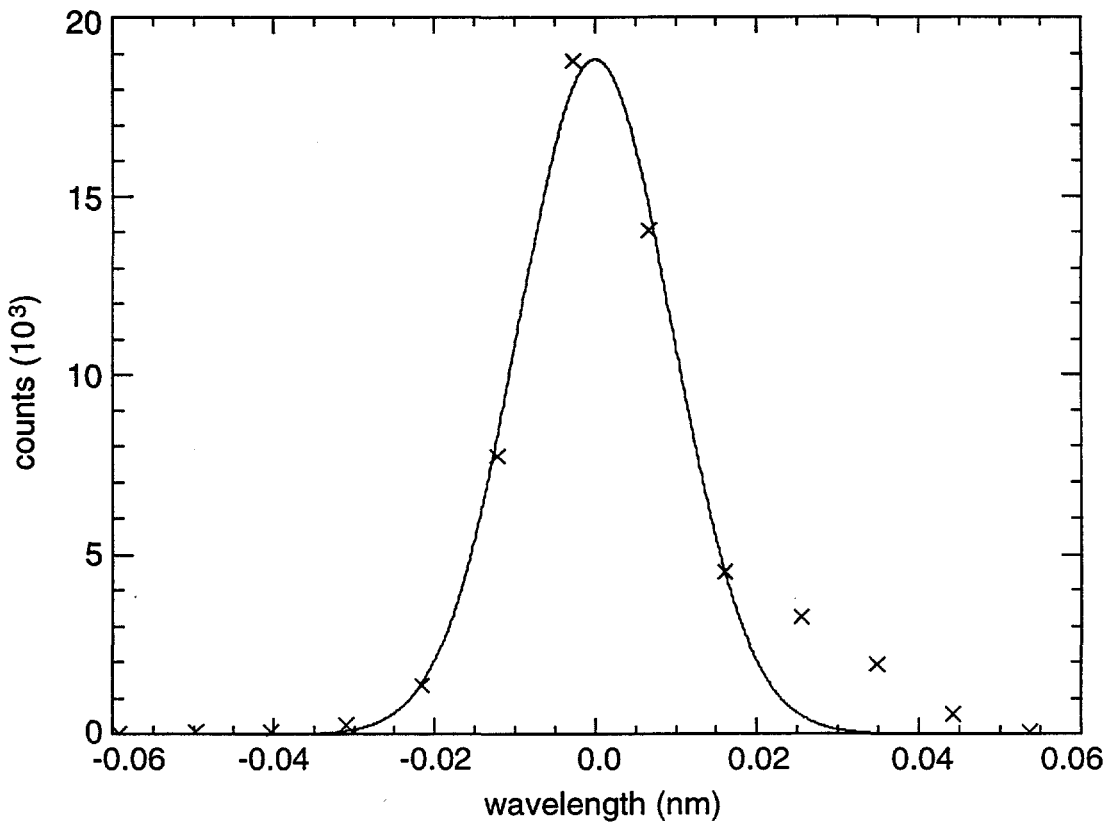


Fig. 7. The Doppler broadened profile of the 206.58 nm B III line from the "offset" end view, $T_i = 14.7$ eV. Note the clear presence of a non-Maxwellian feature on the long wavelength side of the spectrum.

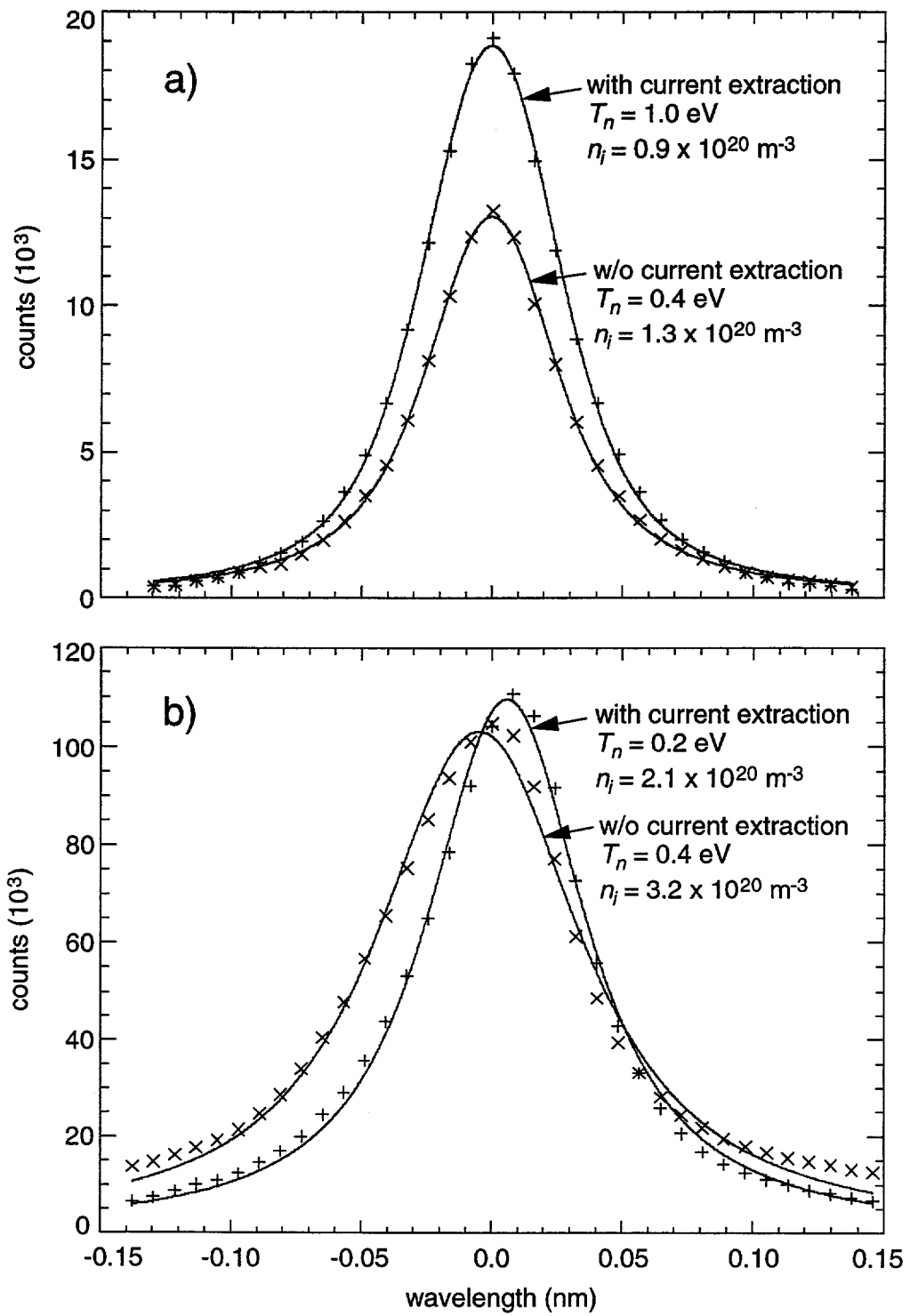


Fig. 8. Comparison of the Voigt profiles of the H_{β} line from the a) side and b) end views, with and without current extraction bias.

In the side view of the plasma from the gun, $T_{n\perp}$ increases and n_i decreases when bias is applied; both fits appear quite good. In the end view, both $T_{n\parallel}$ and n_i appear to decrease when bias is applied to extract current, although changes are small and the fit for biased case is better than for the unbiased case. (The reason for the enhancement of the wings of the distribution in the unbiased case is unknown.) Also, in data from the end view, there appears to be a slight asymmetric enhancement of the short-wavelength side of the neutral hydrogen velocity distribution; this is not apparent in data from the side view. Data from the "offset" end view also show this slight asymmetry. This asymmetry does seem to decrease or disappear altogether in very low power gun discharges. The development of a distinct asymmetry on the short-wavelength side of the line emission profile is apparent as the discharge power is increased from a very low level to normal operational levels. We do not have a definitive explanation for this asymmetry, but it may be evidence for a directed flow of neutral atoms out of gun toward the end view observer.

3.5 Conclusions

These measurements demonstrate that application of current extraction bias to the gun has a positive effect: the ion temperature doubles and the line brightness drops, perhaps indicative of ohmic heating and reduced impurity content. Typical plasma parameters are ion temperatures of 10 to 20 eV with ion densities on the order of 10^{20} m^{-3} . The spatially averaged neutral hydrogen temperature is on the order of 1 eV.

4. SUMMARY

The major impurities in the gun plasma are boron, carbon, and nitrogen from the boron nitride washers and molybdenum from the metal electrodes. The plasma flowing out of the gun is largely uncontaminated by molybdenum; it appears to be trapped in the internal discharge. The gun is able to function as a clean source of high density ($10^{19} - 10^{20} \text{ m}^{-3}$), low temperature ($\sim 10 \text{ eV}$) plasma. When a voltage bias is applied between the gun and some distant current collector, the plasma inside the gun acts a virtual electrode, sourcing up to 1 kA of electron current. Operation of the gun as a virtual electrode actually appears to decrease impurity contamination of the plasma flowing out of the gun, probably because the gun anode is removed from the current return path. A plasma virtual electrode is clearly superior to a metal

electrode when clean emission of a high current density electron current is required.

ACKNOWLEDGEMENTS

This work was supported by the United States Department of Energy. The authors are grateful for the assistance and support of D J Holly, T W Lovell, S Oliva, S C Prager, and M Thomas.

REFERENCES

- [1] G I Dimov and G V Roslyakov, Sov. Pribori. Tech. Exp. **1** (1974) 29.
- [2] G Fiksel, A F Almagri, D Craig, M Iida, S C Prager, and J S Sarff, Plasma Sources Sci. Technol. **5**, 78 (1996); G Fiksel, Ph.D. thesis, University of Wisconsin—Madison (1991).
- [3] D J Den Hartog and D J Holly, “A Simple, Low-cost, Versatile CCD Spectrometer for Plasma Spectroscopy;” to be published in *Review of Scientific Instruments* (January 1997).
- [4] I H Hutchinson, *Principles of plasma diagnostics* (Cambridge University Press, Cambridge, 1987), pp. 216-222.
- [5] Research Systems, Inc, Boulder, Colorado, USA.



EXTERNAL DISTRIBUTION IN ADDITION TO UC-20

S.N. Rasband, Brigham Young University

R.A. Moyer, General Atomics

J.B. Taylor, Institute for Fusion Studies, The University of Texas at Austin

E. Uchimoto, University of Montana

F.W. Perkins, PPPL

O. Ishihara, Texas Technical University

M.A. Abdou, University of California, Los Angeles

R.W. Conn, University of California, Los Angeles

P.E. Vandenplas, Association Euratom-Etat Belge, Belgium

Centro Brasileiro de Pesquisas Fisicas, Brazil

P. Sakanaka, Institute de Fisica-Unicamp, Brazil

Mme. Monique Bex, GANIL, France

J. Radet, CEN/CADARACHE, France

University of Ioannina, Greece

R. Andreani, Associazione EURATOM-ENEA sulla Fusione, Italy

Biblioteca, Istituto Gas Ionizzati, EURATOM-ENEA-CNR Association, Italy

Plasma section, Energy Fundamentals Division Electrotechnical Laboratory, Japan

Y. Kondoh, Gunma University, Kiryu, Gunma, Japan

H. Toyama, University of Tokyo, Japan

Z. Yoshida, University of Tokyo, Japan

FOM-Instituut voor Plasmaphysica "Rijnhuizen," The Netherlands

Z. Ning, Academia Sinica, Peoples Republic of China

P. Yang, Shandong University, Peoples Republic of China

S. Zhu, University of Science & Technology of China, People's Republic of China

I.N. Bogatu, Institute of Atomic Physics, Romania

M.J. Alport, University of Natal, Durban, South Africa

R. Storer, The Flinders University of South Australia, South Australia

B. Lehnert, Royal Institute of Technology, Sweden

Librarian, CRPP, Ecole Polytechnique Federale de Lausanne, Switzerland

B. Alper, Culham Laboratory, UK

A. Newton, UK

2 for Chicago Operations Office

5 for individuals in Washington Offices

INTERNAL DISTRIBUTION IN ADDITION TO UC-20

80 for local group and file